Spin-torque diode frequency tuning via soft exchange pinning of both magnetic layers

A. A. Khudorozhkov, P. N. Skirdkov, and K. A. Zvezdin*
Moscow Institute of Physics and Technology (State University), 141700 Dolgoprudny, Russia;
Russian Quantum Center, 121353 Skolkovo, Moscow, Russia;
and Prokhorov General Physics Institute, Russian Academy of Sciences, 119991 Moscow, Russia

P. M. Vetoshko
Moscow Institute of Physics and Technology (State University), 141700 Dolgoprudny, Russia;
Russian Quantum Center, 121353 Skolkovo, Moscow, Russia;
and Kotel'nikov Institute of Radio-engineering and Electronics (IRE), Russian Academy of Sciences, 125009 Moscow, Russia

A. F. Popkov
Moscow Institute of Physics and Technology (State University), 141700 Dolgoprudny, Russia
and National Research University of Electronic Technology (MIET), 124498 Zelenograd, Moscow, Russia
(Received 31 August 2017; revised manuscript received 30 October 2017; published 8 December 2017)

A spin-torque diode, which is a magnetic tunnel junction with magnetic layers softly pinned at some tilt to each other, is proposed. The resonance operating frequency of such a dual exchange-pinned spin-torque diode can be significantly higher (up to 9.5 GHz) than that of a traditional free layer spin-torque diode, and, at the same time, the sensitivity remains rather high. Using micromagnetic modeling we show that the maximum microwave sensitivity of the considered diode is reached at the bias current densities slightly below the self-sustained oscillations initiating. The dependence of the resonance frequency and the sensitivity on the angle between pinning exchange fields is presented. Thus, a way of designing spin-torque diode with a given resonance response frequency in the microwave region in the absence of an external magnetic field is proposed.

DOI: 10.1103/PhysRevB.96.214410

I. INTRODUCTION

Currently there is much interest in spintronic devices which deal not only with electrons' charge but also with their spins. These devices are expected to surpass conventional electronic devices showing better characteristics and providing new functional capabilities [1–3]. Among these devices are new types of memory [4–6], nanogenerators [7–10], microwave detectors [11–16], magnetic field detectors [17], etc. In particular, one of the most promising spintronic devices is a spin-torque diode based on the magnetic tunnel junction (MTJ) [18,19] and spin-transfer-torque effect [20–25]. It was shown that the application of a radiofrequency (RF) alternating current (ac) can cause the generation of a direct-current (dc) voltage across the structure interface leading to the spin-diode effect [11–14]. Thus, a spin-torque diode can be used for detection of radiofrequency signals [12–15] and even for harvesting their energy [14]. As a consequence, a spin-torque diode should have a high sensitivity, which is the ratio of the incident power to the output dc voltage. Despite the fact that the sensitivity of a spin-torque diode reached only 1.4 mV/mW in the first report [11], the continuous efforts on optimization of the MTJ allowed us to demonstrate the spin-torque diode sensitivity of 12 000 mV/mW [26] under tilted magnetic field applied and even 75 400 mV/mW [27] under zero-bias magnetic field. These results far exceed the sensitivity of the state-of-the-art semiconductor Schottky diode detectors (3800 mV/mW) [26]. However, such high resonant sensitivity has not yet been achieved at resonant frequencies higher than 2–4 GHz. For some applications it is desirable to increase the frequency of the microwave signal [28,29].

In our work we propose a spin-torque diode with magnetic layers softly pinned at some tilt to each other. The possibility of controlling the operating frequency and resonant characteristics of such a spin-torque diode by changing the tilt angle between magnetizations of ferromagnetic layers using the soft exchange pinning of both magnetic layers with additional antiferromagnetic layers (AFM) which have different temperatures of superparamagnetic blocking T_B is considered. This can be done by using AFM layers with different Neel temperature T_N [30], for example, $IrMn_3$ (T_N = 690 K, T_B = 540 K) and FeMn (T_N = 510 K, T_B = 450 K) or the same material but with different thickness [31,32]. In this case it is possible to conduct two-step annealing with different temperatures and different field directions to manufacture device with predetermined tilt angle between AFM pinning.

The strong impact of dc bias on the sensitivity of studied system is observed and the dependence of the sensitivity on the AFM pinning angle is obtained. The relation between the AFM pinning angle and angle between mean magnetizations in FM layers is found, and the key role of magnetostatic interaction is proved.

II. CONSIDERED SYSTEM AND METHOD

The studied structure is a five-layer nanopillar with a diameter of 140 nm composed of an MTJ with two ferromagnetic layers, FM_1 and FM_2, separated by a tunneling barrier MgO and located between two antiferromagnets, AFM_1 and AFM_2 (Fig. 1). Both FM layers are softly pinned by antiferromagnetic layers (AFM_1 and AFM_2) with exchange

*konstantin.zvezdin@gmail.com

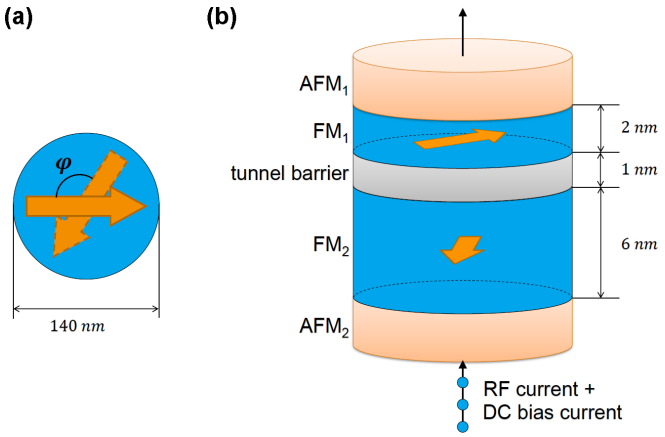

FIG. 1. (a) Top view and (b) side view of the studied structure. Studied nanopillar structure contains an MTJ with two FM layers separated by a MgO tunnel barrier. Both FM layers are softly pinned with AFM layers with exchange bias fields tilted to each other at an angle φ.

bias fields tilted to each other at an angle φ. The thicknesses of FM_1 and FM_2 layers have been chosen to be 2 and 6 nm, respectively, and MgO layer is 1 nm thick. In this case, the effective antiferromagnetic interlayer exchange fields for the FM_1 and FM_2 layers can be estimated as 500 and 167 Oe, respectively. It is worth noting that these pinning exchange fields do not prevent magnetization oscillations with amplitudes sufficient to create overall considerable spin-diode microwave sensitivity. Moreover, the magnetization direction does not match the direction of pinning (this fact is analyzed in detail below). The electric current is applied along the vertical axis perpendicular to the plane of layers (current perpendicular to the plane (CPP) geometry).

The magnetization dynamics in the both FM layer is described by the Landau-Lifshitz-Gilbert (LLG) equation with an additional term responsible for the spin transfer [20,21]:

$$\dot{\mathbf{M}}_i = -\gamma \mathbf{M}_i \times \mathbf{H}^i_{\text{eff}} + \mathbf{T}^i_{\text{STT}} + \frac{\alpha}{M_S}(\mathbf{M}_i \times \dot{\mathbf{M}}_i), \qquad (1)$$

where $\mathbf{M}_i$ is the magnetization vector of the FM_i, γ is the gyromagnetic ratio, α is the Gilbert damping constant, M_S is the saturation magnetization, and $\mathbf{H}^i_{\text{eff}}$ is the corresponding to each layer effective field consisting of a magnetostatic field, an exchange field, an anisotropy field, and an effective antiferromagnetic interlayer exchange field. The spin transfer torque $\mathbf{T}^i_{\text{STT}}$ is represented by two components: a Slonczewski torque (ST) $\mathbf{T}^i_{\text{ST}} = -\gamma f(\theta)\frac{ja_j}{M_S}\mathbf{M}_i \times (\mathbf{M}_i \times \mathbf{m}_j)$ and a fieldlike torque (FLT) $\mathbf{T}^i_{\text{FLT}} = -\gamma j b_j(\mathbf{M}_i \times \mathbf{m}_j)$, where $\mathbf{m}_j$ is a normalized vector along the local magnetization direction of opposite layer and j is the current density along the z direction. The angular dependence of the Slonczewski torque is represented [20,33,34] by $f(\theta) = 2\Lambda^2/[(\Lambda^2+1)+(\Lambda^2-1)\cos\theta]$, where θ is the angle between local magnetizations of the two layers and the Λ^2 parameter characterizes the spacer layer. The ST amplitude is given by $a_j = \hbar P/2heM_S$, where P is the spin polarization of the current, h is the thickness of the free layer, and $e > 0$ is the charge of the electron. The amplitude of the FLT is given by $b_j = \xi_{\text{CPP}} a_j$, where ξ_{CPP} can be larger than 0.4 in the case of an asymmetric magnetic tunnel junction [35]. It is worth noting that all the details of the torque calculation in modeling presented below are similar with widespread micromagnetic solvers (e.g., MuMax [34]).

To investigate the effect of microwave signal rectification we have performed a series of numerical integration of the LLG equation (1) using our micromagnetic finite-difference code SpinPM based on the fourth-order Runge-Kutta method with an adaptive timestep control for the time integration and a mesh size $2.5 \times 2.5 \times h$ nm^3, where h is the corresponding layer's thickness. The FM magnetic parameters used in the modeling are as follows: the saturation magnetization $M_S = 920$ emu/cm^3, the exchange constant $A = 1.3 \times 10^{-6}$ erg/cm, the Gilbert damping factor $\alpha = 0.01$, and the bulk anisotropy is neglected. These parameters are typical for permalloy [36]. The spin polarization of the current is chosen to be $P = 0.4$ [35,36] and the parameter $\Lambda^2 \approx 2.33$, which corresponds to MTJ with TMR 160% [37]. It is worth noting that the reliability of the used method was proved by the fact that several results predicted by our solver for close systems were observed experimentally later [35,36,38].

For the correct processing of simulation results, let us assume that the spin diode is connected to a transmission line and the microwave signal is incident onto it. Then the current density flowing through the MTJ would be $j = j_0 + j_1\cos(2\pi f t)$, where j_0 is the bias current density (dc) and j_1 is the amplitude of the microwave current density (ac) with the frequency f. Due to the telegraph equations, taking into account the impedance matching and assuming that the transmission line is short, the connection between the incident microwave power P_{in} and the power consumed by the spin diode P_0 is the following:

$$P_{\text{in}} = P_0\frac{(R+Z_0)^2}{4RZ_0}, \qquad (2)$$

where R is the time-average spin-diode resistance and Z_0 is the transmission line impedance. The power consumed by the spin diode $P_0 = \langle I^2(t)R(t)\rangle$, where $I = jS$, S is the diode cross-section area, and the brackets $\langle ...\rangle$ denote time averaging. The time-average voltage across the structure could be estimated as $\langle \Delta V\rangle = \langle I(t)R(t)\rangle$. In case of uniformly magnetized FM layers, the dependence of the MTJ resistance R on the angle θ between FM layers' magnetizations could be derived as $R(\theta) = \frac{\bar{R}}{1+\rho\cos\theta}$, where $\bar{R}^{-1} = \frac{R_{\uparrow\uparrow}^{-1}+R_{\uparrow\downarrow}^{-1}}{2}$, $\rho = \frac{R_{\uparrow\downarrow}-R_{\uparrow\uparrow}}{R_{\uparrow\downarrow}+R_{\uparrow\uparrow}}$, and $R_{\uparrow\uparrow}$ and $R_{\uparrow\downarrow}$ are the resistance of the MTJ in parallel ($\theta = 0^{\text{o}}$) and antiparallel ($\theta = 180^{\text{o}}$) states correspondingly [13]. If the magnetization distribution in FM layers is not uniform, then the spatial averaging should be performed. Following previous work [37], we can estimate the spin-diode sensitivity:

$$\varepsilon = \frac{\langle \Delta V\rangle}{P_{\text{in}}} = A\frac{\left\langle \frac{\cos(\omega t)}{1+\rho\cos(\theta(t))}\right\rangle}{\left\langle \frac{\cos^2(\omega t)}{1+\rho\cos(\theta(t))}\right\rangle}, \qquad (3)$$

where $A = \frac{1}{j_1 S}\frac{4RZ_0}{(R+Z_0)^2}$ and $\theta(t)$ is determined in accordance with an LLG equation solution. Here the brackets $\langle ...\rangle$ denote the time and space averaging.

We consider the following parameters of the MTJ in our simulations: cross-section area $S = \pi r^2 = 1.54 \times 10^4$ nm^2,

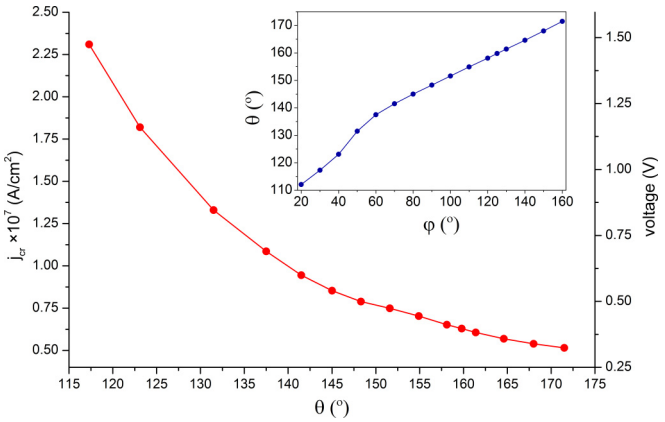

FIG. 2. The dependence of the critical current and corresponding voltage on the angle θ between the mean magnetizations of the FM layers. Inset: The dependence of the angle θ between the mean magnetizations of the FM layers on the AFM pinning angle φ.

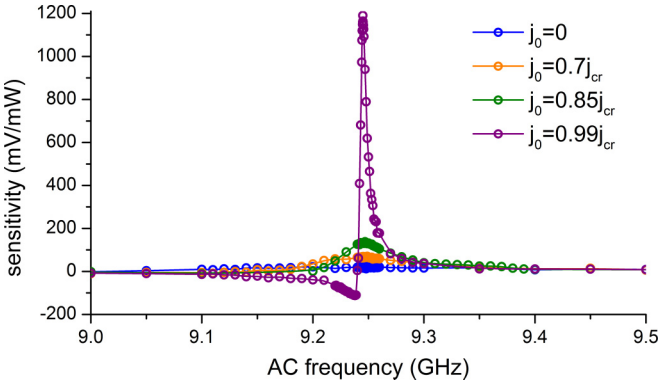

FIG. 3. Spin diode sensitivity depending on microwave current frequency for different values of dc bias currents. AFM pinning angle $\varphi = 120^\circ$.

transmission line impedance $Z_0 = 50\ \Omega$, the average diode resistance $R = 415\ \Omega$, and magnetoresistance $\frac{\Delta R}{R_{\uparrow\uparrow}} = \frac{R_{\uparrow\downarrow} - R_{\uparrow\uparrow}}{R_{\uparrow\uparrow}} = 160\%$. Using it one can find $\rho = 0.44$ and $\Delta R = 369\ \Omega$.

III. MODELLING RESULTS AND DISCUSSION

First, let us analyze equilibrium states of both FM layers. Micromagnetic modeling demonstrates that both layers have quasiuniform magnetization distribution; however, the magnetizations are not collinear to the direction of the AFM pinning at equilibrium, since, besides the effective antiferromagnetic interlayer exchange field, which tends to set magnetization along the AFM pinning direction, there is the magnetostatic effective field, which favors an antiparallel magnetization configuration. The relation between the AFM pinning angle φ and resulting angle θ between mean magnetizations in FM_1 and FM_2 is presented in Fig. 2 (inset). While the angle between the mean magnetization θ only decreases approximately to 110°, the AFM pinning angle φ decreases down to 20°. This means that in the considered case, the magnetostatic effect has a significant impact on the system. At the same time, the $\theta(\varphi)$ dependence is close to linear for φ higher than 60°. Below this point the magnetization distribution is becoming less uniform and nonlinear effects play a significant role.

Further, we investigate the excitation by dc only (in this case $j_1 = 0$). Modelling demonstrates that in a wide range of the AFM pinning angle φ (and corresponding angle θ) there is a critical current j_{cr}, at which the system switches into the autooscillation mode with both FM layers oscillating. The dependence of this critical current and corresponding voltage on the the angle θ between the mean magnetizations of the FM layers is presented in Fig. 2. Below we investigate all the dependencies on the angle φ, since it can be chosen during the annealing in fabrication of the structure. At the same time the real angle between magnetizations θ can be easily identified using $\theta(\varphi)$ dependence from the inset in Fig. 2.

To analyze which of the torques is mostly responsible for magnetization excitation we considered their action on the system separately. For $\varphi = 80^\circ$, $j_0 = 9.5 \times 10^6\ \mathrm{A/cm^2}$ (which is higher than the critical current), and $j_1 = 0$, we have performed two calculations, considering fieldlike torque only ($a_j = 0$, $b_j \neq 0$) and Slonczewski torque only ($a_j \neq 0$, $b_j = 0$). In the first case the transient oscillations subsided to zero in a short time, while in the second case the autooscillations were observed. This demonstrates that the Slonczewski torque plays a leading role in magnetization excitation in the considered structure.

Now let us consider the action of ac with and without bias dc on the example of the case AFM pinning angle $\varphi = 120^\circ$. Here and below, theac current density amplitude was chosen as $j_1 = 10^4\ \mathrm{A/cm^2}$, which corresponds to the power of the incident microwave signal $P_{in} = 10^{-9}$ W. The sensitivity of the spin diode was calculated using Eq. (3) for varied frequencies in the range 9–9.5 GHz for different dc bias currents (below the critical one, which is $j_{cr} = 6.52 \times 10^6\ \mathrm{A/cm^2}$ in this case). The simulation results are presented in Fig. 3. It can be seen that the maximum resonant sensitivity is observed when the dc bias current is slightly below the critical value ($j_0 = 0.99\, j_{cr}$) and the damping is nearly compensated by the spin torque. These results prove that for considered diode dc current even less than critical one can significantly improve the sensitivity (from 20 to 1200 mV/mW in the considered case).

Next we investigate the sensitivity of the MTJ at zero bias current for different AFM pinning angle φ (from 70° to 160°). The results are represented in the inset in Fig. 4. The resonant sensitivity rises when the angle φ decreases, achieving maximum at 60°. At angles about 160° the resonance peak vanishes. At the same time, the maximum value of sensitivity in this case does not exceed 40 mV/mW.

As a final step of the simulation, for each AFM pinning angle φ the dc bias current which is 99% from the critical value has been applied and the sensitivity dependence on microwave signal frequency has been calculated using the formula (3). The results are shown in Fig. 4. The resonance frequency gradually changes as the angle φ between exchange bias fields varies. The maximum sensitivity of 1670 mV/mW is reached at the angle φ of about 125°. As one can see from these results the sensitivity remains rather high down to the angle $\varphi = 70^\circ$. At the same time it is well known [39,40] that the Slonczewski spin-transfer torque (which determines the effect in considered case) becomes ineffective at exciting steady-state magnetic oscillations when the magnetic misalignment is close to 90°,

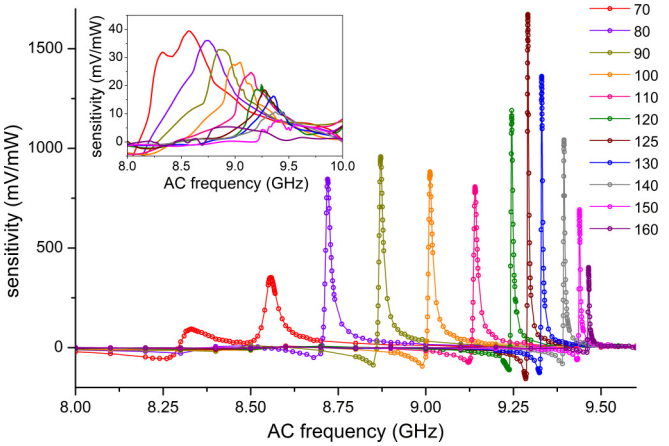

FIG. 4. The dependence of the sensitivity on ac frequency for different AFM pinning angle φ in case of $0.99\,j_{cr}$ bias current. Inset: The dependence of the sensitivity on ac frequency for different AFM pinning angle φ in case of only ac excitation.

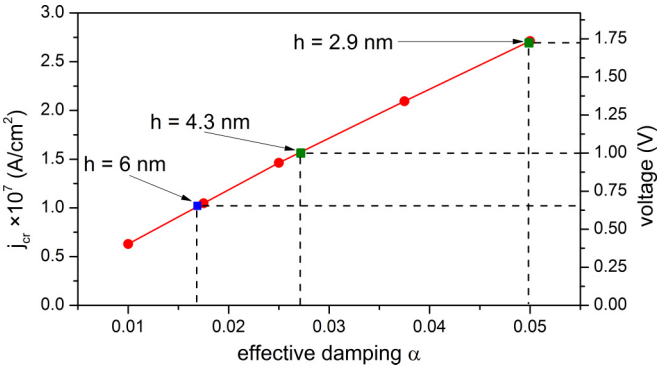

FIG. 5. The dependence of the critical current and corresponding voltage on the effective damping α. Red points represent modeling results, the blue point corresponds to FM_2 with thickness $h = 6$ nm, and green points represent the cases of thickness corresponding to voltages 1 V and 1.7 V, respectively.

and therefore the critical current density should diverge as $1/\cos\theta$ to large magnitudes near this angle. However, there is no contradiction with our results. The considered range of AFM pinning angle φ from 70° to 160° corresponds to the angle θ between the average magnetizations of the FM layers from 141° to 171° (see inset in Fig. 2). Thereby the value of $\theta = 90°$ is simply not achieved, and the angle θ remains always greater than this value. This also explains the fact that we do not observe the inversion of the critical current sign in Fig. 2. These results proves the possibility of production considered spin diodes with predetermined in wide range (from 8.5 to 9.5 GHz) resonant frequency by changing angle φ during the annealing without the significant loss of their performance.

It is important to note that the experimental implementation of the reliably operating spin diode with tilted soft exchange biasing would require significant efforts toward stack design and optimization. For example, exchange biasing to the antiferromagnet can increase the effective damping for a magnetic layer [41,42]. This leads to an increase of the critical current and the corresponding voltage. However, this issue could be addressed in the following ways. Even a slight increase of the thickness of FM layers would result in strong decrease of damping (proportional [41] to the h^{-2}) induced by antiferromagnetic biasing without influencing significantly the magnetization dynamics but only moving the position of the resonance. For instance, if we increase the thickness of the FM_1 from 2 nm only to 2.9 nm and 4.3 nm, then the effective damping already decreases down to $\alpha(2.9\text{ nm}) \approx 0.049$ and $\alpha(4.3\text{ nm}) \approx 0.027$, respectively. The critical currents in this case will be $j_{cr}(2.9\text{ nm}) \approx 2.7 \times 10^7$ A/cm^2 and $j_{cr}(4.3\text{ nm}) \approx 1.56 \times 10^7$ A/cm^2 and corresponding voltage $V(2.9\text{ nm}) \approx 1.7$ V and $V(4.3\text{ nm}) \approx 1$ V (see Fig. 5), which are still reasonable [43]. The effective damping was recalculated to the thickness using experimental results from work [41].

On the other hand, in order to avoid the effect of the growth of magnetic damping due to the exchange pinning of the magnetic layer on the rough surface of the antiferromagnet, one can use synthetic antiferromagnet $AFM_1/FM_0/Ru$ (<1 nm)/FM_1. In this case, there is a sufficiently strong exchange bias acting on the FM_1 layer. Together with that, the linewidth of this magnetic layer, and therefore the effective damping, will be small [44,45]. Moreover, since the rigid fixation of the FM layers magnetization is not required for the operation of considered system, it is possible to use more complex designs of antiferromagnetically coupled soft bias [46] instead of the AFM layer. In this case the effective damping in both FM layers almost does not differ from the damping value for a magnetic layer in isolation.

IV. SUMMARY AND CONCLUSIONS

In summary, the MTJ spin-torque diode with both FM layers softly pinned at different tilt angles by AFMs having different Neel temperatures is proposed. The spin-torque diode effect in such a system and the impact of the dc bias is considered by means of micromagnetic modeling. We demonstrate that the resonance operating frequency of the spin diode with bilateral tilted soft exchange pinning can be significantly higher than that of a traditional spin-torque diode with one pinned layer. We also demonstrate that such a system has sensitivity comparable to the semiconductors in the wide range 8.5–9.5 GHz. Moreover, it is possible to tune the resonant frequency of the diode in this wide frequency range during the manufacturing of the device (by fitting φ during the annealing) without significant loss of the sensitivity. On the other hand, using of voltage-controlled anisotropy instead of bias exchange pinning allows us to change the angle between the equilibrium of magnetizations of the magnetic layers dynamically and therefore to tune the frequency during the operation. The key role of the magnetostatic interaction for the considered system is demonstrated. It is worth mentioning that all results were obtained in the absence of an external magnetic field. The proposed approach can be useful in the engineering of spin diodes for practical applications.

ACKNOWLEDGMENT

The authors acknowledge A. K. Zvezdin for the fruitful discussion. The work was supported by the Russian Science Foundation, Project No. 16-19-00181.

[1] S. Wolf, D. Awschalom, R. Buhrman, J. Daughton, S. Von Molnar, M. Roukes, A. Y. Chtchelkanova, and D. Treger, Science **294**, 1488 (2001).

[2] I. Žutić, J. Fabian, and S. D. Sarma, Rev. Mod. Phys. **76**, 323 (2004).

[3] N. Locatelli, V. Cros, and J. Grollier, Nat. Mater. **13**, 11 (2014).

[4] M. Hosomi, H. Yamagishi, T. Yamamoto, K. Bessho, Y. Higo, K. Yamane, H. Yamada, M. Shoji, H. Hachino, C. Fukumoto *et al.*, in *Proceedings of the IEEE International Electron Devices Meeting* (IEEE, Los Alamitos, CA, 2005), pp. 459–462.

[5] J. Katine and E. E. Fullerton, J. Magn. Magn. Mater. **320**, 1217 (2008).

[6] T. Kawahara, R. Takemura, K. Miura, J. Hayakawa, S. Ikeda, Y. M. Lee, R. Sasaki, Y. Goto, K. Ito, T. Meguro *et al.*, IEEE J. Solid-State Circ. **43**, 109 (2008).

[7] S. I. Kiselev, J. Sankey, I. Krivorotov, N. Emley, R. Schoelkopf, R. Buhrman, and D. Ralph, Nature **425**, 380 (2003).

[8] D. Houssameddine, U. Ebels, B. Delaët, B. Rodmacq, I. Firastrau, F. Ponthenier, M. Brunet, C. Thirion, J.-P. Michel, L. Prejbeanu-Buda *et al.*, Nat. Mater. **6**, 447 (2007).

[9] V. Pribiag, I. Krivorotov, G. Fuchs, P. Braganca, O. Ozatay, J. Sankey, D. Ralph, and R. Buhrman, Nat. Phys. **3**, 498 (2007).

[10] D. V. Dimitrov, X. Peng, S. S. Xue, and D. Wang, Spin oscillator device, U.S. Patent No. 7,589,600. 15 Sep. 2009.

[11] A. Tulapurkar, Y. Suzuki, A. Fukushima, H. Kubota, H. Maehara, K. Tsunekawa, D. Djayaprawira, N. Watanabe, and S. Yuasa, Nature **438**, 339 (2005).

[12] Y. Suzuki and H. Kubota, J. Phys. Soc. Jpn. **77**, 031002 (2008).

[13] C. Wang, Y.-T. Cui, J. Sun, J. Katine, R. Buhrman, and D. Ralph, J. Appl. Phys. **106**, 053905 (2009).

[14] O. Prokopenko, I. Krivorotov, E. Bankowski, T. Meitzler, S. Jaroch, V. Tiberkevich, and A. Slavin, J. Appl. Phys. **111**, 123904 (2012).

[15] O. V. Prokopenko, I. N. Krivorotov, T. J. Meitzler, E. Bankowski, V. S. Tiberkevich, and A. N. Slavin, in *Magnonics* (Springer, Berlin, 2013), pp. 143–161.

[16] A. Jenkins, R. Lebrun, E. Grimaldi, S. Tsunegi, P. Bortolotti, H. Kubota, K. Yakushiji, A. Fukushima, G. De Loubens, O. Klein *et al.*, Nat. Nanotechnol. **11**, 360 (2016).

[17] P. Braganca, B. Gurney, B. Wilson, J. Katine, S. Maat, and J. Childress, Nanotechnology **21**, 235202 (2010).

[18] D. D. Djayaprawira, K. Tsunekawa, M. Nagai, H. Maehara, S. Yamagata, N. Watanabe, S. Yuasa, Y. Suzuki, and K. Ando, Appl. Phys. Lett. **86**, 092502 (2005).

[19] S. Yuasa, T. Nagahama, A. Fukushima, Y. Suzuki, and K. Ando, Nat. Mater. **3**, 868 (2004).

[20] J. C. Slonczewski, J. Magn. Magn. Mater. **159**, L1 (1996).

[21] L. Berger, Phys. Rev. B **54**, 9353 (1996).

[22] M. Tsoi, A. G. M. Jansen, J. Bass, W.-C. Chiang, M. Seck, V. Tsoi, and P. Wyder, Phys. Rev. Lett. **80**, 4281 (1998).

[23] E. Myers, D. Ralph, J. Katine, R. Louie, and R. Buhrman, Science **285**, 867 (1999).

[24] J. A. Katine, F. J. Albert, R. A. Buhrman, E. B. Myers, and D. C. Ralph, Phys. Rev. Lett. **84**, 3149 (2000).

[25] G. Fuchs, N. Emley, I. Krivorotov, P. Braganca, E. Ryan, S. Kiselev, J. Sankey, D. Ralph, R. Buhrman, and J. Katine, Appl. Phys. Lett. **85**, 1205 (2004).

[26] S. Miwa, S. Ishibashi, H. Tomita, T. Nozaki, E. Tamura, K. Ando, N. Mizuochi, T. Saruya, H. Kubota, K. Yakushiji *et al.*, Nat. Mater. **13**, 50 (2014).

[27] B. Fang, M. Carpentieri, X. Hao, H. Jiang, J. A. Katine, I. N. Krivorotov, B. Ocker, J. Langer, K. L. Wang, B. Zhang *et al.*, Nat. Commun. **7**, 11259 (2016).

[28] L. Fu, Y. Gui, Y. Xiao, M. Jaidann, H. Guo, H. Abou-Rachid, and C. Hu, in *SPIE Defense+ Security* (International Society for Optics and Photonics, Washington, 2015), p. 945406.

[29] L. Fu, Y. Gui, L. Bai, H. Guo, H. Abou-Rachid, and C.-M. Hu, J. Appl. Phys. **117**, 213902 (2015).

[30] A. Popkov, N. Kulagin, and G. Demin, Solid State Commun. **248**, 140 (2016).

[31] B. Negulescu, D. Lacour, F. Montaigne, A. Gerken, J. Paul, V. Spetter, J. Marien, C. Duret, and M. Hehn, Appl. Phys. Lett. **95**, 112502 (2009).

[32] A. Devasahayam and M. Kryder, J. Appl. Phys. **85**, 5519 (1999).

[33] J. Xiao, A. Zangwill, and M. D. Stiles, Phys. Rev. B **70**, 172405 (2004).

[34] A. Vansteenkiste, J. Leliaert, M. Dvornik, M. Helsen, F. Garcia-Sanchez, and B. Van Waeyenberge, Aip Advances **4**, 107133 (2014).

[35] A. Chanthbouala, R. Matsumoto, J. Grollier, V. Cros, A. Anane, A. Fert, A. V. Khvalkovskiy, K. A. Zvezdin, K. Nishimura, Y. Nagamine, H. Maehara, K. Tsunekawa, A. Fukushima, and S. Yuasa, Nat. Phys. **7**, 626 (2011).

[36] A. Dussaux, B. Georges, J. Grollier, V. Cros, A. Khvalkovskiy, A. Fukushima, M. Konoto, H. Kubota, K. Yakushiji, S. Yuasa *et al.*, Nat. Commun. **1**, 8 (2010).

[37] N. Kulagin, P. Skirdkov, A. Popkov, K. Zvezdin, and A. Lobachev, Low Temp. Phys. **43**, 708 (2017).

[38] N. Locatelli, A. Hamadeh, F. A. Araujo, A. D. Belanovsky, P. N. Skirdkov, R. Lebrun, V. V. Naletov, K. A. Zvezdin, M. Muñoz, J. Grollier *et al.*, Sci. Rep. **5**, 17039 (2015).

[39] F. Mancoff, R. Dave, N. Rizzo, T. Eschrich, B. Engel, and S. Tehrani, Appl. Phys. Lett. **83**, 1596 (2003).

[40] D. C. Ralph and M. D. Stiles, J. Magn. Magn. Mater. **320**, 1190 (2008).

[41] T. Mewes, R. Stamps, H. Lee, E. Edwards, M. Bradford, C. Mewes, Z. Tadisina, and S. Gupta, IEEE Magn. Lett. **1**, 3500204 (2010).

[42] S. M. Rezende, A. Azevedo, M. A. Lucena, and F. M. De Aguiar, Phys. Rev. B **63**, 214418 (2001).

[43] C. P. S. d. Silva, Tunnel barrier dielectric breakdown and endurance in magnetic tunnel junctions, Ph.D. thesis, University of Lisbon, 2010.

[44] B. Khodadadi, Investigation of magnetic relaxation mechanisms and dynamic magnetic properties in thin films using ferromagnetic resonance (FMR) technique, Ph.D. thesis, University of Alabama, 2016.

[45] J. Chen, J. Feng, and J. Coey, Appl. Phys. Lett. **100**, 142407 (2012).

[46] C. Shang, D. Mauri, K. San Ho, A. G. Roy, and M. Mao, Antiferromagnetically-coupled soft bias magnetoresistive read head, and fabrication method therefore, U.S. Patent No. 8,611,054. 17 Dec. 2013.